

## Article

# Towards Sustainable Material: Optimizing Geopolymer Mortar Formulations for 3D Printing: A Life Cycle Assessment Approach

Charlotte Roux <sup>1,\*</sup> , Julien Archez <sup>2</sup> , Corentin Le Gall <sup>2</sup>, Myriam Saadé <sup>2</sup> , Adélaïde Féraïlle <sup>2</sup> and Jean-François Caron <sup>2</sup> 

<sup>1</sup> MINES Paris—PSL Research University, CEEP (Centre Energie Environnement Procédés), 60 Boulevard Saint Michel, 75006 Paris, France

<sup>2</sup> Navier Laboratory, Ecole des Ponts ParisTech, Gustave Eiffel University CNRS, 77454 Champs sur Marne, France

\* Correspondence: charlotte.roux@minesparis.psl.eu

**Abstract:** Geopolymer-based concretes have been elaborated among others for their potential to lower the environmental impact of the construction sector. The rheology and workability of fresh geopolymers make them suitable for new applications such as 3D printing. In this paper, we aim to develop a potassium silicate- and metakaolin-based geopolymer mortar with sand and local earth additions suited for 3D printing and an environmental assessment framework for this material. The methodology aims at the optimization of both the granular skeleton and the geopolymer matrix for the development of a low-environmental-impact material suited for 3D printing. Using this approach, various metakaolin/earth geopolymer mortars are explored from a mechanical and environmental point of view. The environmental assessment of the lab-scale process shows an improvement for the climate change category but a degradation of other indicators, compared to Portland-cement-based concrete. Several promising options exist to further optimize the process and decrease its environmental impacts. This constitutes the main research perspective of this work.

**Keywords:** sustainable material; geopolymers; 3D printing; material characterization; environmental optimization; life cycle assessment



**Citation:** Roux, C.; Archez, J.; Le Gall, C.; Saadé, M.; Féraïlle, A.; Caron, J.-F. Towards Sustainable Material: Optimizing Geopolymer Mortar Formulations for 3D Printing: A Life Cycle Assessment Approach. *Sustainability* **2024**, *16*, 3328. <https://doi.org/10.3390/su16083328>

Academic Editors: Uroš Klanšek and Tomaž Žula

Received: 13 March 2024

Revised: 9 April 2024

Accepted: 12 April 2024

Published: 16 April 2024



**Copyright:** © 2024 by the authors. Licensee MDPI, Basel, Switzerland. This article is an open access article distributed under the terms and conditions of the Creative Commons Attribution (CC BY) license (<https://creativecommons.org/licenses/by/4.0/>).

## 1. Introduction

Concrete is responsible for 8% of global greenhouse gas (GHG) emissions and 5.2% of particulate matter (PM<sub>10</sub>) emissions [1]. With the gradual awareness of the urgency of decarbonizing the concrete and cement industries, alternatives have been developed, particularly to replace Portland cement, which largely contributes to the carbon footprint of concrete [2,3]. Some alternatives rely on the replacement of cement using by-products of high-emitting industries such as coal and steel production, providing fly ashes and slags, respectively. Other emerging technologies aim at reducing emissions and energy use in cement production [4,5]. The wide adoption of such technologies, however, faces multiple barriers, ranging from regulatory issues to supply, product confidence, and technical obstacles [6].

In addition to being a major contributor to climate change, concrete production also consumes notable amounts of natural resources such as aggregates and sand with a certain quality. The world consumption of sand and aggregates is estimated to reach about 41 billion tons per year and is expected to increase soon [7]. The sand supply has long been taken for granted but nowadays faces issues of local resource depletion, impacts on the ecosystem, and climatic instabilities [8].

In this context, geopolymers recently benefited from renewed interest. Geopolymers (GPs) are inorganic, amorphous three-dimensional alumino-silicate materials synthesized at

an ambient temperature through the activation of an aluminosilicate source (i.e., metakaolin) by an alkaline solution [9]. The polycondensation reaction between alumina and silicates occurring under basic alkali activation results in a geopolymer network. Such geopolymer provides resistance to high temperatures, as well as high mechanical or chemical resistance due to GP covalent bonds [10,11]. Sodium and potassium alkaline solution are largely used as activators but another synthesis path involving phosphoric acid is also studied, to a lesser extent [12].

Geopolymers are seen as an alternative to Ordinary Portland Cement (OPC), with expected lower CO<sub>2</sub> emissions [9]. Portland cement requires heating up to 1450 °C for several hours which causes the calcination of the limestone (clinkerization process). The combustion of fuels to reach such a temperature and the decarbonization of limestone both emit a high quantity of CO<sub>2</sub>—about one ton of CO<sub>2</sub> per ton of cement [13]. In comparison, geopolymer production requires the use of a chemical solution of alkali silicates and the heating of kaolin clay at a lower temperature (around 850 °C), without the calcination of limestone. The synthesis of raw material is, therefore, less emitting than the Portland cement production process, when considering the CO<sub>2</sub> emitted directly during the production process [9]. However, its environmental advantage has to be rigorously confirmed in a life cycle and multi-criteria perspective [14].

Life Cycle Assessment (LCA) is a method currently widely used to assess the environmental impacts of products and services [15,16]. It is a multi-step and multi-criteria approach developed to avoid impacts shifting along the value chain and among impact categories. Multiple Life Cycle Assessment studies have been applied to geopolymer (GP) matrices, concretes, and mortars, with the latter being constituted of a geopolymer matrix and a granular skeleton [17–22]. So far, no scientific consensus has been reached about their environmental performances, mainly because the results highly depend on the formulation and raw materials used for their synthesis. Some authors show a significant reduction of environmental impacts when using GP concrete based on slag, fly ash, and alkali-silicate systems [18,23], while others confirm a slight reduction of GHG emissions using fly ash and blast-furnace geopolymers [19]. They also highlight a trade-off between impacts on climate change and other environmental categories such as abiotic resources, eutrophication, and acidification, for which GP concrete presents higher impacts. GP concrete could even have a higher carbon footprint than conventional concrete depending on upscaling commercial scenarios for 3D printing concrete [24].

Most studies agree on the importance of the contribution to the impacts of alkali activator production. To reduce the contribution of the geopolymer matrix, fillers such as sand can be added to form the geopolymer mortar. Another way is to use raw earth instead of sand [25] as GP chemistry makes it more prone to interact with the earth, especially clays, than ordinary concrete [26,27]. In this way, from a circular economy perspective, geopolymer synthesis could help recover excavated earth.

In addition to their potential intrinsic environmental performances, GP mortars could be suited for 3D printing. Applied to the construction sector, this technique, currently under development, is considered as a way to reduce the amount of construction materials used [28]. Geopolymers present a totally different physic than 3D-printed rock analogs [29] and a different setting than cement mortars—they are closer to polymeric glues than hydrated mortars. They also may be highly completed with different fillers. For these reasons, they become good challengers for this new way of building. Their interesting durability properties would also be relevant in a growing number of applications (structural materials, heat-resistant pavement, sewer pipes, sub-aqueous seawater, etc.) [30]. Improved knowledge of geopolymers is thus broadly recommended to understand their potential to mitigate carbon emissions in the construction sector [31–33] and precisely evaluate the domain of environmental relevance for this technology. Specific work on geopolymer mortars for 3D printing shows low embodied carbon per m<sup>3</sup> compared to cementitious material [34]. However, the contribution of transport and the curing and mixing process are not clearly presented. Moreover, most formulations reviewed are based on used fly ash

and blast-furnace slags (Table 1), which are by-products of polluting industries and are only available in limited quantities. Even if the use of fly ash and blast-furnace slags could be envisioned in countries where electricity is still mainly coal-based, they remain by-products. They might not be a long-term option for replacing cementitious blends on a large scale. The development of a potassium silicate- and metakaolin-based geopolymer mortar with low environmental impact, sufficient mechanical properties, and suitability for 3D printing could therefore be beneficial for the construction sector. Its environmental impact must, however, be thoroughly studied using a comprehensive Life Cycle Assessment.

**Table 1.** Comparison of embodied GHG emissions for GP concrete or mortar and Ordinary Portland Concrete found in the literature.

Geopolymer (GP) Description	GHG Emissions of GP (kgCO <sub>2</sub> eq/m <sup>3</sup> )	GHG Emissions of Ref. OPC (kgCO <sub>2</sub> eq/m <sup>3</sup> )	Ref	Comments
Binder, suitable for 3D printing—FA50% + GGBS50%	107	556	[34]	Carbon accounting and not full LCA (f.e. water carbon footprint is set to zero). Reference binder is 80% OPC and 20% FA.
Binder, suitable for 3D printing—FA78.5% + GGBS13.8% + SF7.7%	134	556	[34]	Carbon accounting and not full LCA (f.e. water carbon footprint is set to zero). Reference binder is 80% OPC and 20% FA.
Slag and FA GP binder for 3D printing	677	493	[24]	Full, complete LCA, including sensitivity analysis on allocations.
“Standard” FA GP concrete	320	354	[35]	Carbon accounting and not full LCA.
FA GP concrete	169	306	[19]	Also investigating MK-GP, but clear figures are not available. MK-GP impacts are higher than FA-GP impacts.
FA and slag GP cement	267	895	[18]	Indian context, cement and not concrete.

FA: Fly ash, GGBS: granulated blast-furnace slag.

The objective of this paper is to propose a formulation for a low-environmental-impact geopolymer mortar to be used for 3D-printing applications exploiting locally available materials. The research explores a lab-scale process developed in a French context. After a brief description of the studied class of geopolymer, the article describes the LCA-based approach used to optimize geopolymer formulation, relying on its environmental performance. An initial formulation of a geopolymer mortar is tested, and its environmental impacts are evaluated to identify the life cycle stages with the main impact. The article then presents the results of formulation optimization using LCA and examines the influence of LCA parameters such as transport. Based on a comparison of three 3D-printing materials, it discusses potential improvements of the process to further decrease the environmental impacts of metakaolin geopolymers, highlighting the need to improve the accuracy of LCA data.

## 2. Materials and Methods

### 2.1. Methodological Approach

Our methodological approach is summed up in Figure 1. To understand the environmental impacts of a printable geopolymer formulation, a first environmental assessment was led using a GP matrix previously developed in the NAVIER laboratory and suitable for 3D printing, as described in [36]. This first matrix serves as a reference for further optimization. It is composed of 46%w metakaolin, 37%w potassium alkaline solution, 15%w wollastonite, and 2%w glass fibers and will be called GP-GfW in this study.

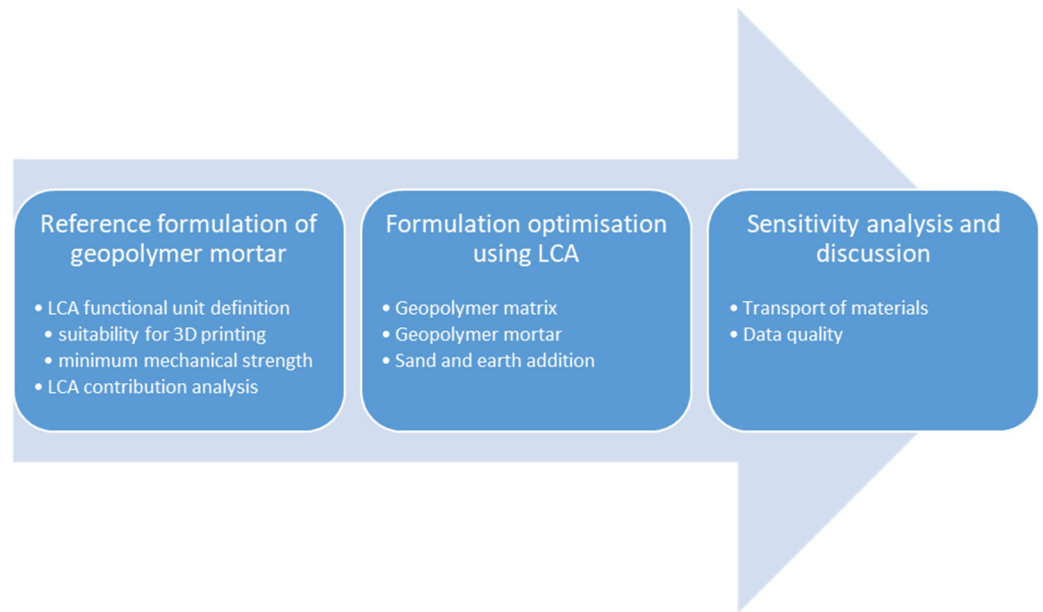


**Figure 1.** Methodological approach.

Based on the environmental impact of a geopolymer-based 3D-printing material, an optimization of the matrix was undertaken to lower the environmental impacts while maintaining sufficient mechanical property. Then, geopolymer formulations (matrix + granular skeleton) were developed to decrease GHG emissions while maintaining printability and a minimum mechanical strength of 32.5 MPa (NF-EN 197-1 standard [37]).

The results were further analyzed to understand the influence of certain parameters on the environmental impacts of the formulation. The studied process is a lab process and is not optimized as the processes currently in place within the cement and concrete sector are. Transport distances and modes were investigated in a sensitivity analysis to understand how impacts could be decreased by a scale effect. The poor quality of some data, related to low temporal representativity, for instance, is also discussed.

## 2.2. Raw Materials and Sample Preparation

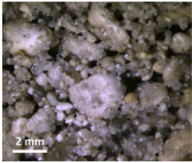
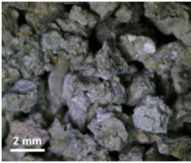
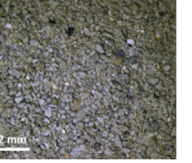
### 2.2.1. Raw Materials

Geopolymer formulations were synthesized at the NAVIER laboratory with potassium silicate solution (Geosil14515:  $[K] = 7.0 \text{ M}$ ,  $\text{SiO}_2 = 19\%w$ ,  $\text{K}_2\text{O} = 22\%w$  and  $\text{H}_2\text{O} = 59\%w$ ) and metakaolin aluminosilicate source (M1000:  $\text{SiO}_2: 55\%w$   $\text{Al}_2\text{O}_3: 40\%w$ ,  $D50 = 10 \mu\text{m}$ ) [38]. The developed formulations differ from most GPs presented in the literature, which are sodium silicate solution and industrial waste (fly ashes, ground granulated blast slag)-based GPs [39]. Given their limited availability on the French territory and the uncertainties of their future supply, industrial wastes were not included in the tested formulations.

A granular skeleton constituted partly of masonry sand (0–4 mm diameter) and partly of raw earth was then added to the geopolymer matrix to form a geopolymer mortar. Raw earth was supplied locally from the excavation works of the “Grand Paris” project. The earth was dried in an oven (24 h at 100 °C) and then sieved consecutively into four particle sizes (1.6–2.5 mm, 0.8–1.6 mm, 0.4–0.8 mm, and <0.4 mm). Qualitative tests regarding earth addition in geopolymers showed water absorption issues. The earth has a higher water demand than sand due to the presence of clays (like illite or smectite for the earth used in this study), especially for the low granulometry (<0.8 mm). To quantify the water absorption, the water demand of earth particles and sand was quantified by measuring the quantity of water (in increments of 10  $\mu\text{L}$ ) to be added to 10 g of material to reach a moist state. The moist state corresponds to a visual criterion where the sand or earth is fully wet. Their values are reported in Table 2. Given that the earth absorbs most of the water from the mix, the mortar becomes dry too quickly and the earth addition becomes

impossible. The absorption of water by the earth modifies the ratio of chemical components and consequently the polycondensation reaction of the geopolymer.

**Table 2.** Granulometry and water demand of sand and earth used in this study.

Particle Type	Sand		Earth		
Grain size (mm)	0–4	1.6–2.5	0.8–1.6	0.4–0.8	<0.4
Water absorption $\pm 0.02$ (mL/g)	0.13	0.06	0.28	0.58	0.75
Picture					

To optimize the earth quantity, the granular skeleton of the mix was improved following the Fuller-Thompson method [36], considering Equation (1).

$$p_i = (d_i/D)^{0.45} \quad (1)$$

where  $p_i$  is the percent passing  $i$ th sieve,  $d_i$  (mm) is the opening size of the  $i$ th sieve, and  $D$  (mm) is the maximum particle size.

An optimized granularity was designed to compensate for the high water absorption of the small earth fractions (diameter under 0.8 mm). The final composition consisted of sand for aggregates with a diameter lower than 0.8 mm and earth for coarse aggregates, with a size grain higher than 0.8 mm. The optimized grain size distribution is exposed in Figure 2.

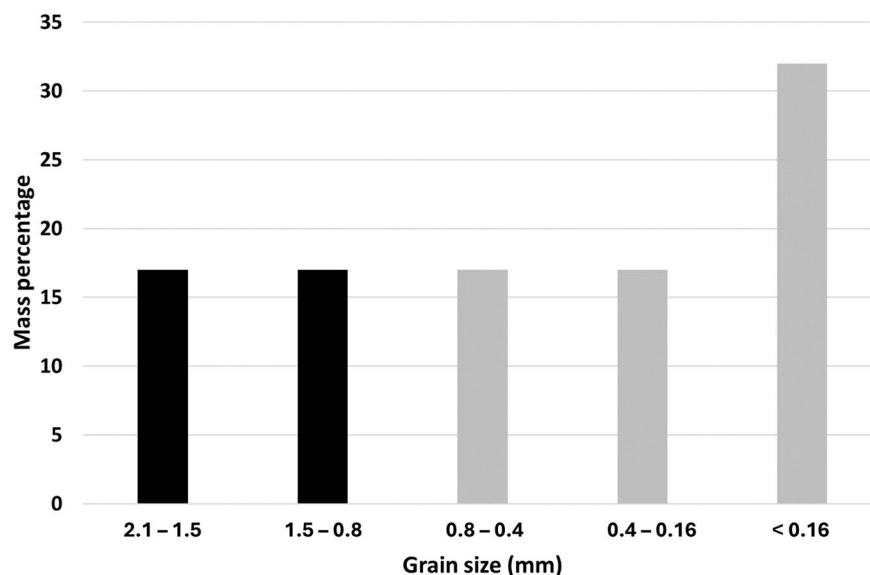


**Figure 2.** Grain size distribution of ■ earth and ■ sand in the optimized granularity.

### 2.2.2. Sample Preparation

The nomenclature used in this work is  $M_aS_bSa_yE_z$ , where  $a$  and  $b$  characterize the ratio between potassium silicate solution (S) and metakaolin (M), so  $a + b = 100\%$ . Moreover, “ $y$ ” and “ $z$ ” represent, respectively, the quantity in grams of sand (Sa) and earth (E) added to form the geopolymer mortar for 100 g of geopolymer paste ( $a + b$ ). The sample preparation consisted of adding metakaolin into a silicate solution progressively while mixing with a planetary mixer. After 3 min of mixing, sand and/or earth were added progressively to the

geopolymer paste and mixed for 5 min. The sample was then cast in a  $40 \times 40 \times 160$  mm closed mold and the bubbles were removed with a vibrating needle (50 Hz, 1 min). The samples were demolded after 24 h and stored in a sealed plastic bag. The printability of the sample was quantified by overlaying manually the material with a syringe with a 15 mm diameter. The normal compressive strengths were evaluated after 7 days on 12 (half 40-40-160 mm) samples using an MTS with a 100 kN load cell at 0.5 mm/min constant speed.

### 2.3. Environmental Characterization

#### 2.3.1. Environmental Assessment: Methodological Choices and Perimeter of the LCA for 3D Printing Geopolymer Mortars

**Definition of the functional unit:** The functional unit is defined as: “producing  $1 \text{ m}^3$  of geopolymer mortar suitable for 3D printing”. The impact of the formulation or 3D-printing process on the mechanical properties of these geopolymers has already been studied in the past [40], and according to the NF EN 197-1 standard, the compressive strength of the mortar should reach at least 32.5 MPa to ensure its suitability for 3D printing. The material printability also needs to be assured. Such printability was qualified by manually overlaying the material with a syringe, as a preliminary test [38].

**System boundaries:** The flowchart of the system is presented in Figures 3 and 4. The study is a cradle-to-gate assessment, and we included in the system the production of GP mortar as well as upstream activities and processes. GP applications are not considered, and consequently, neither are transportation, use, and end-of-life. The equipment used to process the materials (e.g., mixing unit, oven, molds) and the land occupation generated by the lab were also excluded from the system processes, as no data were accessible. Moreover, no material loss during the process was accounted for in this study. To consider the localized characteristic of this supply, LCA data were as much as possible adapted to the French context.

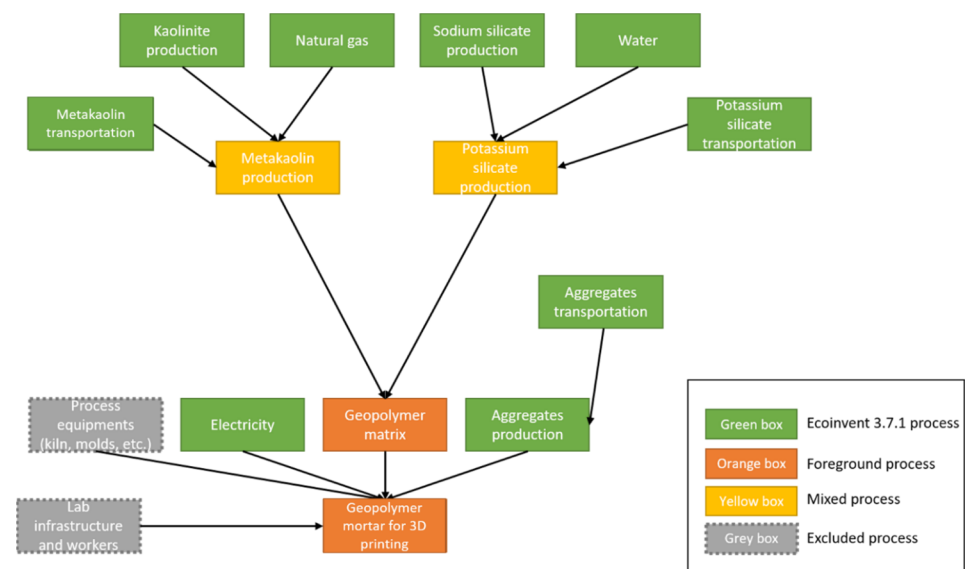


**Figure 3.** Granularity flowchart of the GP studied system. Mixed processes are ecoinvent processes adapted or modified for the study. Foreground processes are processes defined by the authors.

The study was led using the open-source framework Brightway 2 and its graphic interface Activity-Browser [41,42], relying on the database Ecoinvent 3.7 Cutoff [43,44].

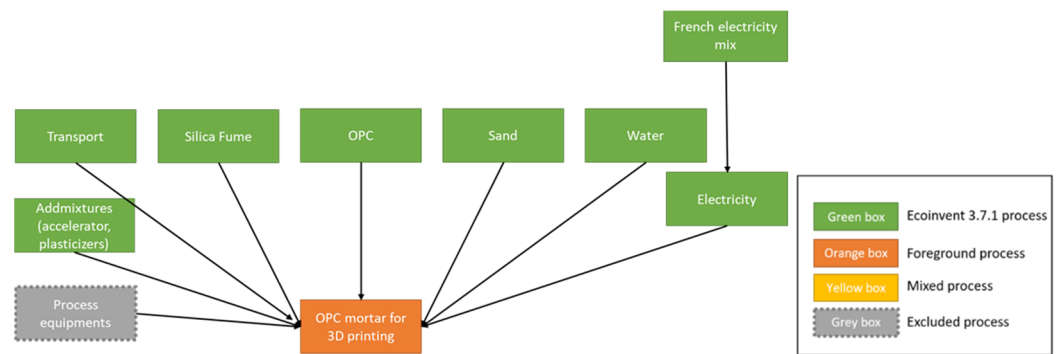


**Figure 4.** Flowchart of the OPC studied system. Mixed processes are ecoinvent processes adapted or modified for the study. Foreground processes are processes defined by the authors.

### 2.3.2. Life Cycle Inventory of Individual Processes

The assumptions made to derive the process inventory for each component of the studied system are exposed below. Exhaustive information on the system modeling is given in Supplementary Materials, Section S1.

**Metakaolin (MK):** The considered metakaolin (MK) was provided by the French company Ceradel under the label METAKAOLIN ARGICAL M1000 (Ceradel, Clérac, France). According to commercial communication by Imerys, it was assumed that the MK was formed from a process involving high-purity kaolinite heated at 750 °C in a rotary kiln. The modeling process considers 1.16 kg of kaolin production (ecoinvent process, contextualized using a French electricity mix) and 2.5 MJ of natural gas heating to obtain 1 kg of metakaolin [22].

**Potassium silicate solution (PSS):** The potassium silicate solution (PSS) used in this process is a commercial solution distributed by the German chemical company Woellner (Ludwigshafen, Germany), under the name Geosil 14515. An existing process in the ecoinvent database for sodium silicate was selected based on the same synthesis process (hydrothermal). A molar equivalent was applied in the ongoing flows, to replace sodium with potassium [45]. This process had a close solid ratio with the product Geosil 14515 used in this study (48% mass of dried content compared to 45% for this study). Finally, water flow was added to the process to match the dried content of the Geosil 14515. This way of designing a process for PSS was confirmed by the industrial producer.

**Glass fiber:** Previously introduced in a formulation developed in the NAVIER laboratory and suitable for 3D printing [36], glass fibers were used in our reference formulation. The glass fiber came from a French producer located in the south of France (700 km from the lab), and the global market in the ecoinvent database was adjusted accordingly. A French electricity mix was considered for glass fiber production.

**Wollastonite:** Wollastonite production is not represented in the ecoinvent database. It is usually a mined stone, although it can be artificially produced. Here, only open mining was considered, using the asbestos chrysotile global production process as a reference. Transport distances were also adjusted, as the lab providers are located in Mexico.

**Other raw materials:** The other constituents were directly taken from the ecoinvent 3.7 databases. If possible, data for the French context were taken. When not available, Swiss (CH) or European (RER) data were considered.

**Transportation of the matrix components:** The transportation process was directly extracted from the Ecoinvent 3.7 library database without changes. We used the EURO4 class for all transportation vehicles (trucks). For PSS and MK, distances between the actual production sites and the NAVIER laboratory were calculated. The following driving distances were estimated using Google Maps:

- MK: Clérac—Champs sur Marne: 535 km.
- PSS: Ludwigshafen—Champs sur Marne: 504 km.

For the supply of cement, sand, and gravel, distances were estimated. A distance of 50 km was taken to account for displacement from the cement factory to the lab. This estimated distance is about 30 km for the aggregates (sand and gravel).

As the GP mortar was synthesized at the laboratory scale, and given the small number of required materials, it was considered that the vehicles used belonged to the 3.5–7.5 T category, for MK, G, and aggregates. As the process for Ordinary Portland Concrete (OPC) is more usual, 16–62 T lorries were considered for its transportation.

Electricity: The electricity consumption of the process was evaluated at 4 kWh per m<sup>3</sup> of produced concrete or mortar. This value is an expert-based estimation for regular concrete provided by the French National Project RECYBETON (<https://www.pnrecybeton.fr/> accessed on 11 April 2024). It should be studied in more depth and adapted to GPs in further research. The French low-voltage market for electricity included in Ecoinvent v3.7.1 was chosen for the inventory.

### 2.3.3. Environmental Indicators

The main environmental issue usually related to traditional concrete and mortar is its impact on climate change (CC). This environmental category is thus a major focus of this study. Nevertheless, other impact categories (listed in Table 3) were examined to provide an overview of the environmental profile of the GP technology and avoid impact shifting.

**Table 3.** Abbreviations and units of the environmental indicator used in this study.

Impact Category	Abbreviation	Unit
Climate Change Total	CC	kg CO <sub>2</sub> -eq
Freshwater and Terrestrial Acidification	FTA	mol H <sup>+</sup> -eq
Freshwater Ecotoxicity	Fex	CTUe
Freshwater Eutrophication	Feu	kg P-eq
Marine Eutrophication	Meu	kg N-eq
Terrestrial Eutrophication	Teu	mol N-eq
Carcinogenic Effects	CE	CTUh
Ionizing Radiation	IR	kg Bq U <sup>235</sup>
Non-Carcinogenic Effects	nCE	CTUh
Ozone Layer Depletion	OD	kg CFC-11-eq
Photochemical Ozone Creation	POCP	kg NMVOC eq
Respiratory Effects, Inorganics	RE	disease incidences
Resources, Dissipated Water	DW	m <sup>3</sup> water deprived
Resources, Fossils	RF	Megajoule
Resources, Land Use	RLU	soil quality index—dimensionless
Resources, Minerals, and Metals	RMM	kg Sb-Eq
Cumulative Energy Demand	CED	MJ-Eq

The LCA was first performed using the European consensus set of environmental indicators reached around the International Life Cycle Data initiative (ILCD). The midpoint set of indicators from the methodology ILCD 2.0 2018 was used [46,47]. To give an overview of the impact at the damage level to raise potential impact shifting among categories, a second assessment was performed using the ReCiPe2016, hierarchist method [48].

Although the cumulative energy demand is sometimes depreciated by LCA experts and seen as additional information more than a full LCA indicator [49], it was still added to the midpoint indicators because of its very frequent use in the construction sector. This set of impact categories aims to provide a comprehensive overview to avoid or at least quantify the phenomena of pollution transfers and impact shifts.

## 3. Results

### 3.1. Environmental Impact Assessment of Elementary Processes of Geopolymer Mortars and Reference Situation

In order to identify the parameters to be further optimized, a first environmental assessment of the reference formulation (GP-GfW) was performed. The impact factors of

the elementary processes of the geopolymer production system used for the calculation are available in Supplementary Materials, Section S2. The contribution analysis of this formulation is exposed in Figure 5. Although the additions (wollastonite and glass fiber) are not negligible, the main driver for environmental impact in most categories is the potassium silicate solution (PSS), followed by the metakaolin and transport. The electricity contribution appears to be negligible in this study.

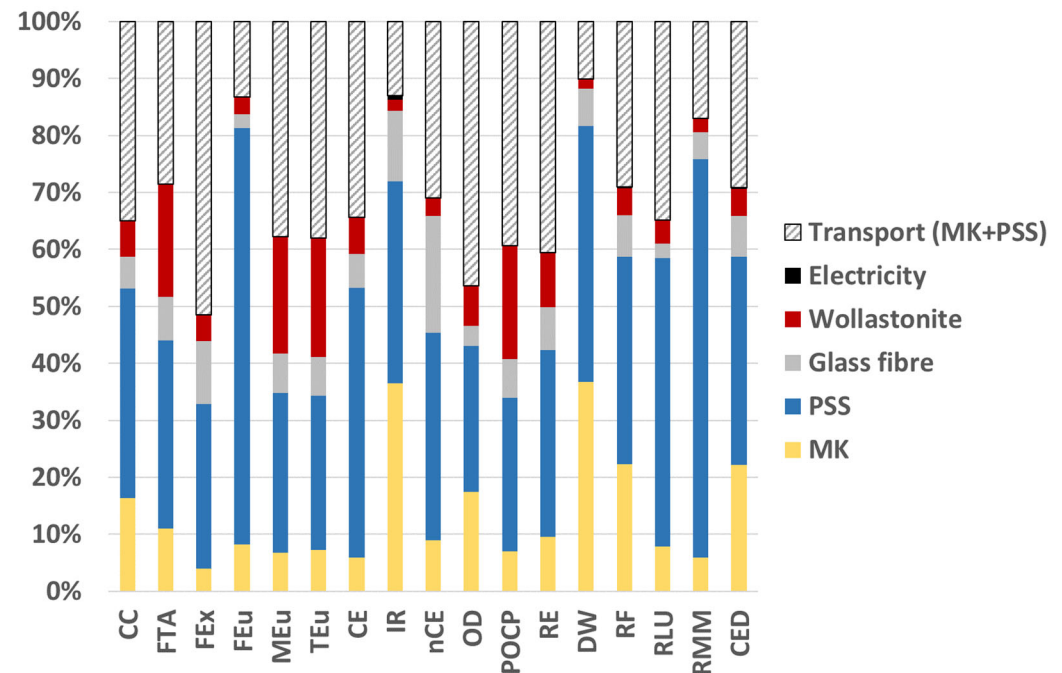


**Figure 5.** Reference situation for 3D-printing geopolymer formulation. CC = climate change, FTA = freshwater and terrestrial acidification, Fex = freshwater ecotoxicity, Feu = freshwater eutrophication, Meu = marine eutrophication, Teu = terrestrial eutrophication, CE = carcinogenic effect, IR = ionizing radiation, nCE = non-carcinogenic effects, OD = ozone depletion, POCP = photochemical ozone creation, RE = respiratory effects, DW = water depletion, RF = fossil resources, RMM = minerals and metals resources, CED = cumulative energy demand.

### 3.2. Optimization of the Geopolymer Formulation to Lower GHG Emissions

Based on the preliminary LCA results, the optimization of the matrix is undertaken to lower the quantity of PSS while maintaining sufficient mechanical properties. A formulation that lowers the matrix quantity by integrating a maximum of sand and earth additions and is suitable for the 3D-printing process was then developed and characterized mechanically.

#### 3.2.1. The Geopolymer Matrix

In order to obtain a geopolymer formulation adapted for 3D printing with sufficient compressive strength and low GHG emissions, the geopolymer matrix was first optimized. Different ratios of metakaolin/potassium silicate solution were investigated with a metakaolin mass percentage ranging from 40 to 60%. The mechanical curves obtained for a M<sub>50</sub>S<sub>50</sub> geopolymer are displayed in Figure 6a. This formulation exhibits a 60 ± 3 Mpa compressive strength and a brittle failure. The compressive strength and the climate change impact, expressed in kgCO<sub>2</sub>eq/m<sup>3</sup> of the different geopolymer matrices are presented in Figure 6b. The compressive strength presents small variations but stays in the same order of magnitude (from 51 to 60 Mpa). When the metakaolin content increases from 40 to 50%, the compressive strength slightly increases due to enhanced polycondensation reaction [50]. It then slightly decreases with a further increase in metakaolin content, from 50 to 60%, probably because of the presence of unreactive particles and a decrease in the paste workability [51]. The climate change impact per m<sup>3</sup> increases slightly with increased

PSS content. Indeed, the PSS has a bigger impact per mass unit than metakaolin (0.63 and 0.58 kgCO<sub>2</sub>eq/kg, respectively, for the M<sub>40</sub>S<sub>60</sub> and M<sub>60</sub>S<sub>40</sub> formulations). However, the density of the matrix increases with the decreased proportion of PSS which leads to an increase in impact per volume unit. Since the values of climate change impact are of the same order of magnitude, the M<sub>50</sub>S<sub>50</sub> matrix presenting better mechanical properties seems optimal. In terms of buildability, printing tests show that every tested geopolymer matrix is not adapted for 3D printing because the paste flows when several layers are stacked during printing. Their yield stress has then to be increased to improve the buildability, which means to be able to carry the weight of the layers [52]. For that purpose, it is possible to add reinforcement elements such as glass fibers or wollastonite [38] or to change the volume fraction by adding, for instance, sand or earth [53].

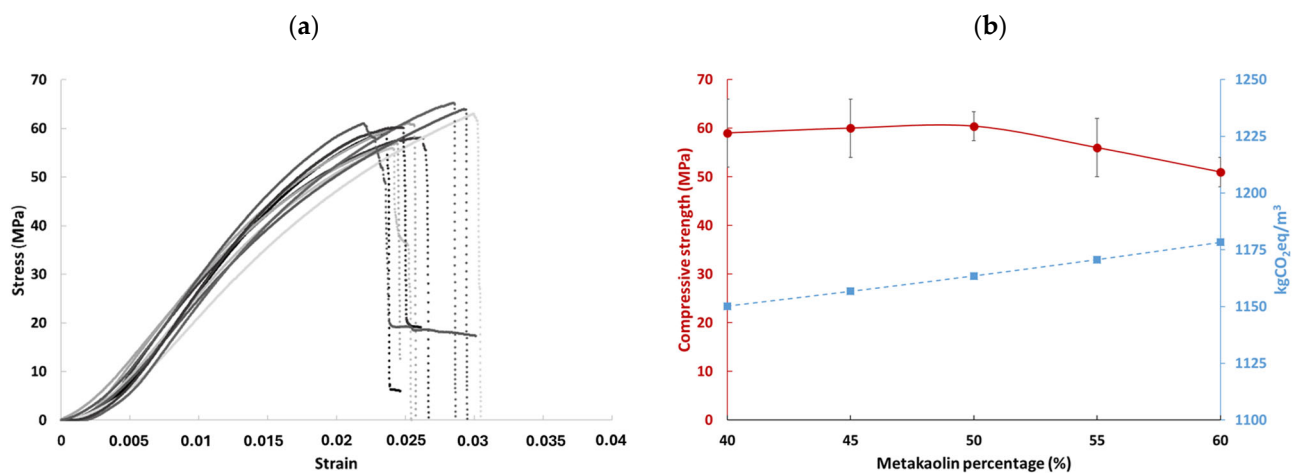


**Figure 6.** (a) Compressive curves of a M<sub>50</sub>S<sub>50</sub> geopolymer and (b) • compressive strength and ■ climate change in kgCO<sub>2</sub>eq/m<sup>3</sup> as a function of metakaolin percentage in the geopolymer matrix.

### 3.2.2. The Geopolymer Mortar

In order to decrease the matrix quantity and increase the buildability, sand was added to the different geopolymer matrices. To define the maximum quantity of sand to be added, two thresholds were determined. The first threshold corresponds to the quantity of sand for which the mortar begins to shear under mixing. After reaching this threshold, sand was continuously added to a point where a vibrating needle could not fluidize the mix anymore. The admissible range of sand quantity suitable for 3D printing lies between these two thresholds; before the first, the mortar is not stackable, and after the second, the mortar is not pumpable. These two thresholds are presented in Figure 7a for the different geopolymer binders. The thresholds are almost similar for a quantity of metakaolin ranging from 40 to 50% of the binder. With higher proportions of metakaolin, a saturation level is reached, and the value of the second threshold decreases. In that range, the water coming from the silicate solution is not sufficient in the geopolymer matrices, and the amount of sand it is possible to add decreases.

To ensure that the geopolymer mortar formulations are mechanically reliable, the compression strength of the M<sub>60</sub>S<sub>40</sub> geopolymer binder was measured. This is reported in Figure 7b as a function of the quantity of added sand. The mechanical strength decreases slightly from 51 ± 3 MPa without sand to 44 ± 2 MPa with the addition of sand (M<sub>60</sub>S<sub>40</sub>Sa<sub>60</sub>). Consequently, the addition of sand to form a printable geopolymer mortar has no significant effects on the properties of the material.

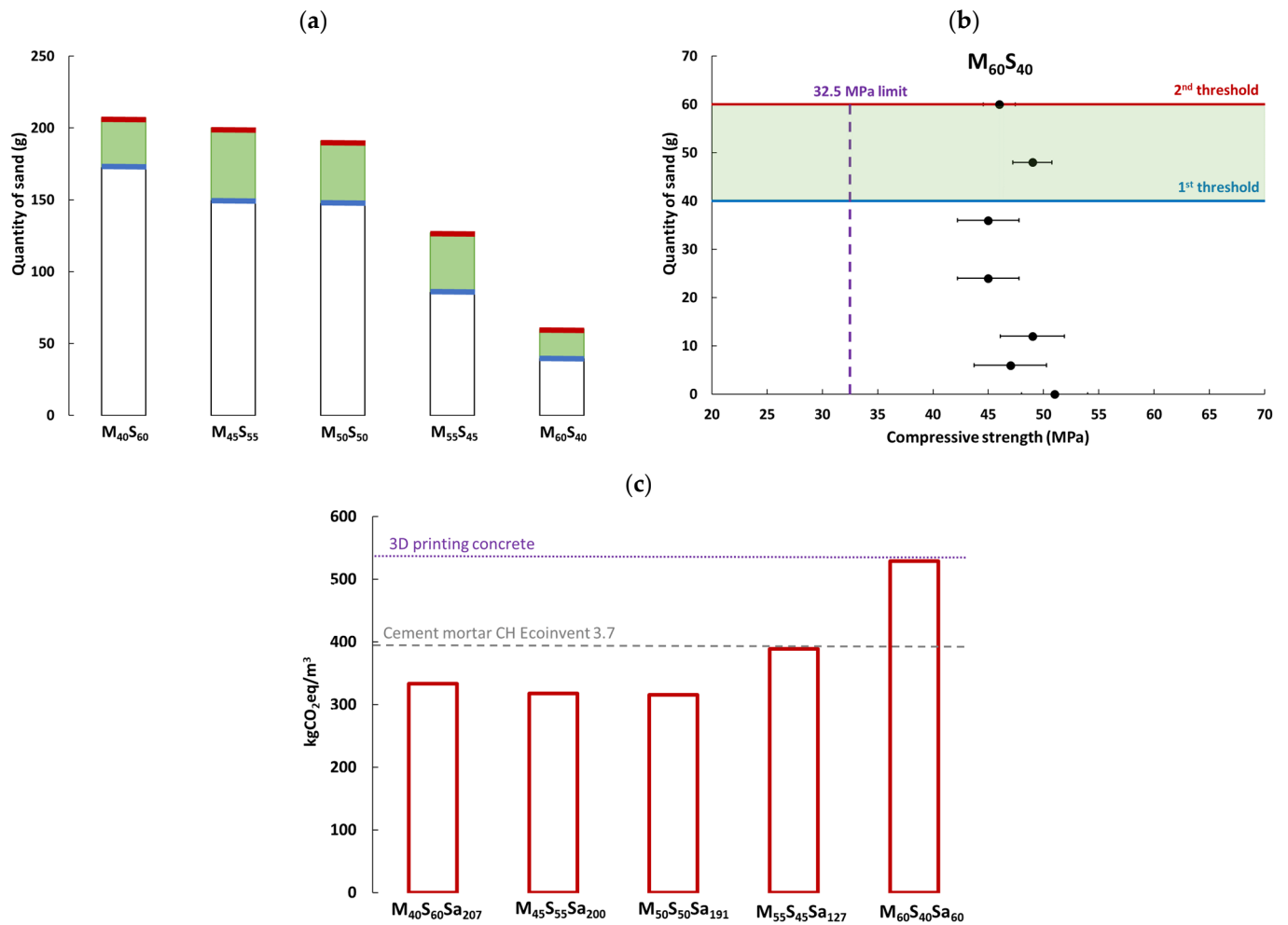


**Figure 7.** (a) quantity of sand added in different geopolymer matrices with the (■) printable domain between the ■ first and ■ second thresholds (b) quantity of sand as a function of compressive strength for an  $M_{60}S_{40}$  formulation and (c) quantity of  $\text{kgCO}_2/\text{m}^3$  for the second threshold mortar formulations.

The value of climate change impact per volume unit ( $\text{kgCO}_2\text{eq}/\text{m}^3$ ) was then calculated for mortar formulations at the second threshold and is reported in Figure 7c. The climate change impact decreases slightly with a decrease in silicate solution until it reaches an optimum at  $316 \text{ kgCO}_2\text{eq}/\text{m}^3$  for the  $M_{50}S_{50}Sa_{191}$  formulation. It increases afterward. This optimum can be explained by two phenomena: (i) the silicate solution has a big impact on climate change and (ii) the formulation that contains a high quantity of silicate solution allows us to add more sand, which decreases the final impact. The impact of the  $M_{50}S_{50}Sa_{191}$  formulation is 3.7 times lower than the ( $M_{50}S_{50}$ ) matrix impact. The addition of sand in the geopolymer formulation then drastically decreases the climate change impact of geopolymers per unit of volume. Nevertheless, their impact depends on the quantity it is possible to add to the GP matrix. Moreover, the geopolymer formulations with high silicate content ( $M_{40}S_{60}Sax$ ,  $M_{45}S_{55}Sax$ ,  $M_{40}S_{60}Sax$ ) have climate change impacts lower than 3D-printed concrete ( $529 \text{ kgCO}_2\text{eq}/\text{m}^3$ ) or generic mortar ( $393 \text{ kgCO}_2\text{eq}/\text{m}^3$ ) while keeping sufficient mechanical properties (above 40 MPa). These formulations can then be selected to progress toward a sustainable material for 3D printing.

### 3.2.3. Optimization with Earth Addition

After optimizing the geopolymer formulation through the addition of sand, tests were conducted using the mix of earth and sand determined in Figure 1. This mix was added

in a 1:1 mass proportion with an M<sub>50</sub>S<sub>50</sub> geopolymer matrix to obtain a printable material (M<sub>50</sub>S<sub>50</sub>Sa<sub>66</sub>E<sub>34</sub>). The printability and buildability of this formulation were tested with a manual extrusion tool, as shown in Figure 8a. As shown in previous work [38], this preliminary test provides an indication of the buildability of the material.

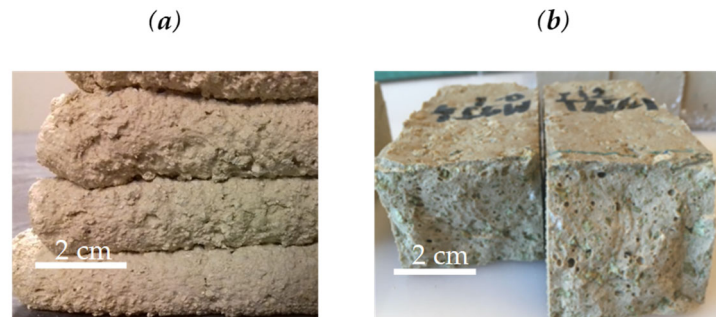


**Figure 8.** Photos of (a) printed layers of the earth-sand-M50S50Sa66E34 mix extruded with a manual tool and (b) a 40 × 40 × 160 mm sample.

The tested formulation presents a compressive strength equal to  $31 \pm 4$  MPa. This is lower than the geopolymer matrix due to the earth's inclusion (Figure 8b) and a modification of the polycondensation reaction. However, it is still acceptable for construction applications. These results show that the optimization of the granular skeleton allows us to add local earth into the formulation to improve the circular economy while keeping sufficient mechanical properties and obtaining a mix adapted for 3D printing.

### 3.3. Comparison of the Optimized Geopolymer Formulation with Other Printing Materials

The environmental performance of the optimized formulations as printing materials was assessed in a comparative approach at a material scale. The robotic process necessary to print the material [54–56] was excluded from the scope of the study. The formulation with the addition of sand (M<sub>50</sub>S<sub>50</sub>Sa<sub>191</sub>—GP-S) and the formulation with the addition of earth and sand (M<sub>50</sub>S<sub>50</sub>Sa<sub>66</sub>E<sub>34</sub>)—GP-SE were compared to two other 3D-printing formulations—one based on Portland cement [54], named 3DCM, and one based on a geopolymer [36], with glass fibers and wollastonite additions (GP-GfW). The four formulations are summarized in Table 4.

**Table 4.** Formulation of the 3D-printing mortars.

Quantity (in kg/m <sup>3</sup> )	3D Cement Mortar—«3DCM» [54]	Quantity (in kg/m <sup>3</sup> )	GP Mortar «GP-GfW» [36]	GP Mortar «GP-S» (Section 3.2.2)	GP Mortar «GP-SE» (Section 3.2.3)
OPC	540	MK	915.4	327.4	505
Silica Fume	480	PSS	736.3	327.4	505
Sand	1033	Sand	0	1248.8	666.6
Water	212	Wollastonite	298.5	0	0
Accelerator	6	Glass fibers	39.8	0	0
Plasticizers	8.8	Steamed earth	0	0	333.3

Considering the Portland cement-based mortar 3DCM, most upstream requirements are accounted for in the market processes of the ecoinvent databases. Electricity consumption for the 3D cement mortar was added considering 4 kWh/m<sup>3</sup> and transport is also accounted for, using the process “market for concrete, 50 MPa, global” contextualized to Europe. The 4 scenarios are considered to have equivalent properties in terms of mechanical resistance, pumpability and extrudability, making them suitable for 3D printing in the

perspective of structural uses. Relative results are provided for a clearer interpretation of the results, 3D cement mortar (3DCM) being the reference/denominator (Figure 9).

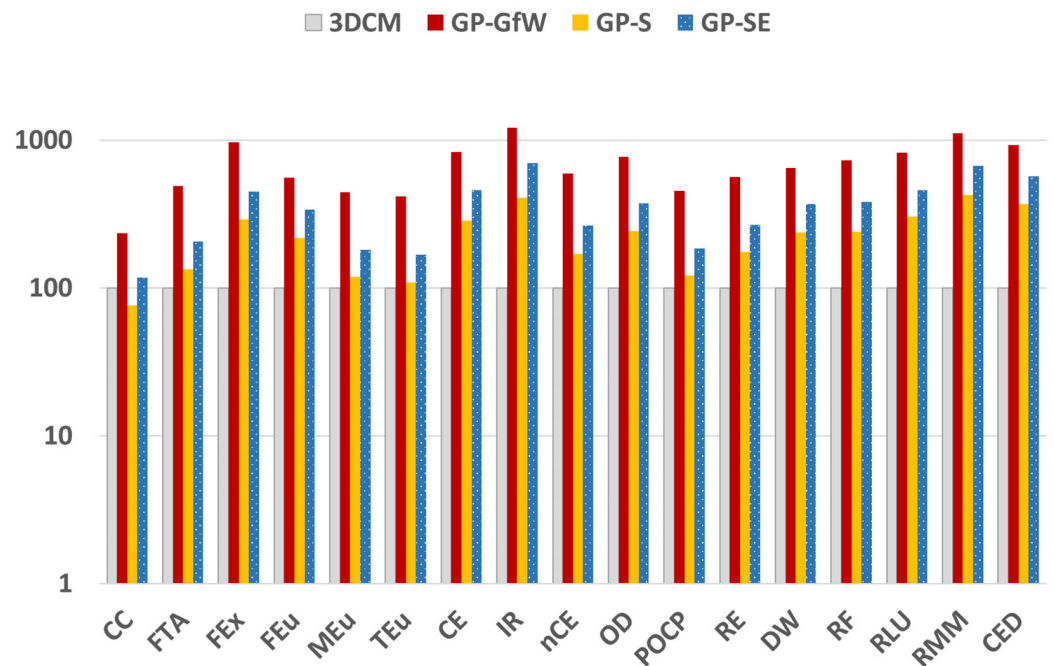


**Figure 9.** LCA of GP-S and GP-SE mortar, compared to 3DCM (used as reference, fixed at 100%) and GP-GfW (log scale).

With the currently tested formulations and in a French context, the results show that the GP formulations present impacts equivalent to or higher than 3DCM, except for climate change, for which GP-S has a lower impact (−23%). Secondly, the GP-S and GP-SE perform significantly better than the previous formulation with a higher share of the matrix (GP-GfW). However, GP-SE does not perform better than GP-S due to a higher matrix proportion. The climate change impact of geopolymer mortar highly depends on its formulation—whether by the nature or quantity of its raw material or by the optimization of the granular skeleton.

Figure 10 shows the important contribution of transportation of the material for GP mortar: from 7 to 47% according to certain categories (28% on average). The same figures for 3DCM vary from 4 to 42% (16% on average). This is related to the lab-scale and poor development of production sites for kaolinite. Another source of improvement clearly stands in the material production itself: PSS and MK productions are significant contributors to most categories, and further research should investigate the improvement of the production process, especially on toxicity-related impacts for PSS. Further effort to decrease the needed matrix quantity would also be very efficient as it will decrease both impacts from production and transport.

Figure 11 shows the contribution of different environmental issues to damage to human health, biodiversity, and resources, using the ReCiPe2016 method endpoint level. If climate change clearly dominates human health, other categories are not negligible, such as toxicity (cancer and non-cancer) and particulate matter (which can be associated with “respiratory effects”). On the biodiversity side, global warming dominates, followed by terrestrial acidification, photochemical ozone formation, and land use. A multi-criteria assessment is therefore essential to clearly prove the environmental relevance of the technology, restricting the evaluation to carbon footprint is not sufficient and could lead to impact shifting.

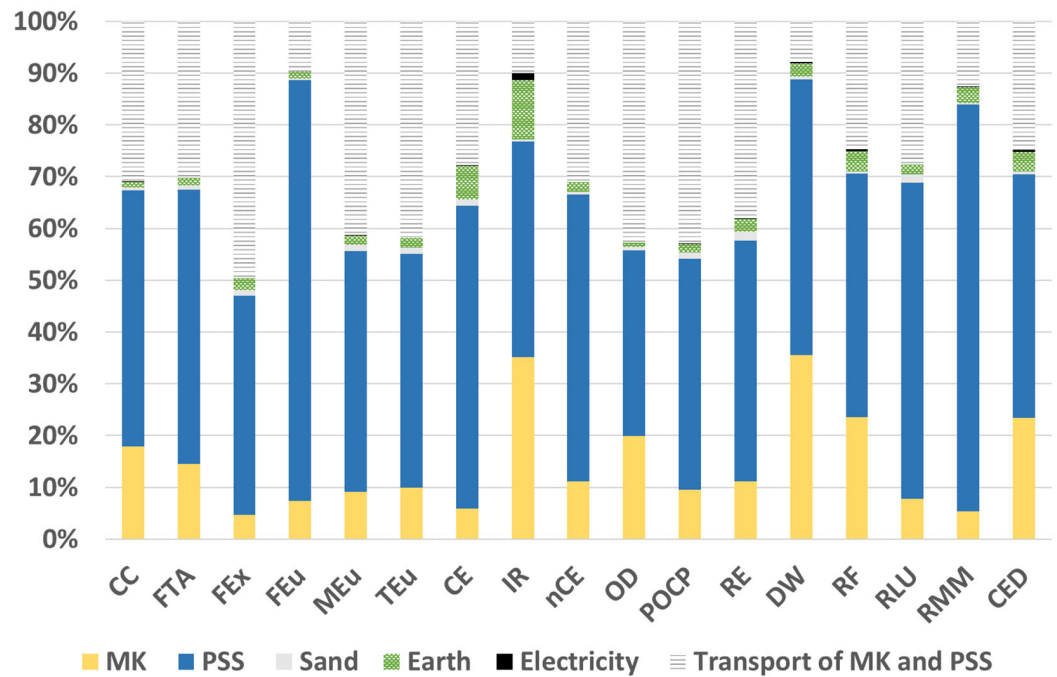


Figure 10. Contribution analysis of GP-SE mortar.

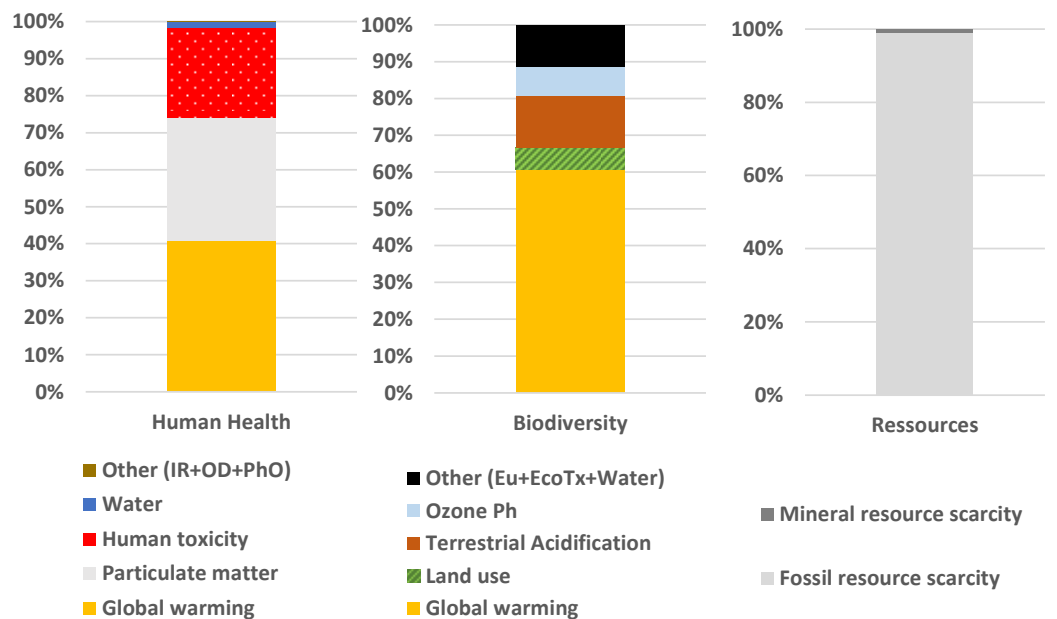


Figure 11. Midpoint contribution to Endpoint for GP-S concrete, Human Health (left), Biodiversity (center), and resource (right) using ReCiPe2016, hierarchist method.

Results for the GP materials are largely hampered by scale factors, as we compared a lab-scale technology to a fully deployed technology that has benefited from many years of innovation and improvements, and its small-scale production units are close to final users. Consequently, these direct results are to be taken with caution. A scale-up of the GP technology will help assess its long-term potential. It should cover both the possible optimization of the geopolymer elaboration process (equipment efficiency, raw materials) and the overall value chain (optimization of transport type and distance). This is a major perspective of this work and is further detailed in the Section 4.

## 4. Discussion

### 4.1. Value Chain Optimization

The developed process is currently an under-optimized laboratory process compared to well-established conventional materials such as concrete mortars. This explains why the impact of transport is so high compared to 3DCM. To account for this bias, a sensitivity analysis was performed on transport type and transport distances; first, we improved transport to 16–32 T EURO6 lorries (scenario T++) and secondly, we decreased transport distances from 500 km to 50 km for MK and PSS (scenario T++D−). The results are presented in Figure 12 below, which provides a selection of seven indicators among the most important ones according to the endpoint assessment.

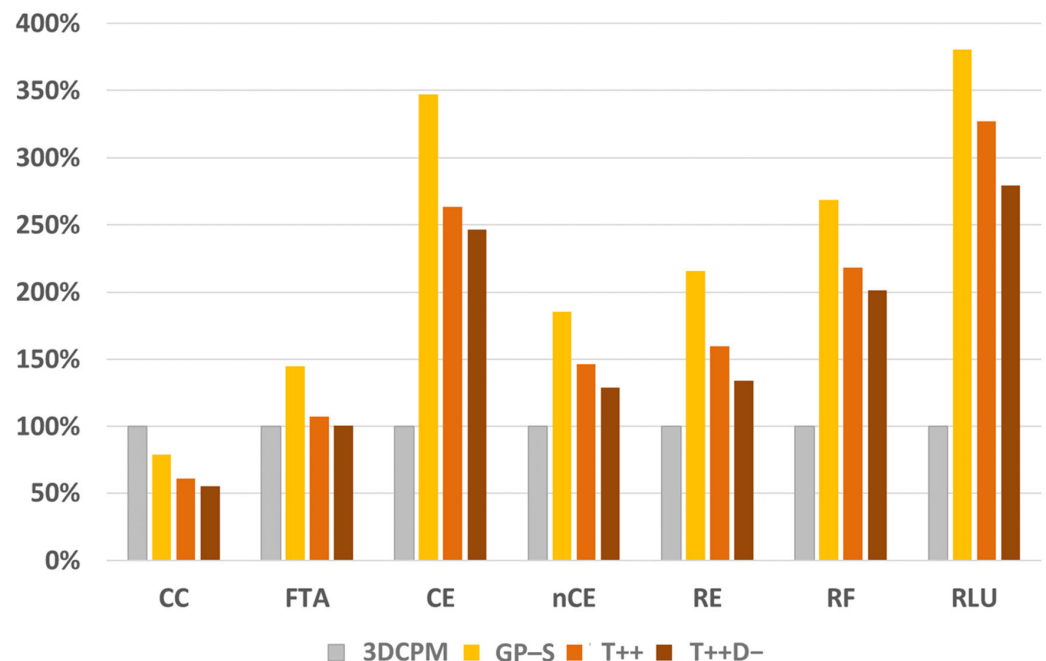


**Figure 12.** Assessment of the reference lab process and scale-up scenarios, midpoint level, considering 3DCM mortar as a baseline scenario.

There is great room for improvement, which could be made thanks to the scale effect. This limited analysis based on only two parameters should be further investigated to produce full scale-up scenarios, focusing both on process optimization and distribution options. Process improvements can be obtained thanks to bigger and more efficient equipment, such as MK flash calcination [57,58], a change in energy suppliers, or a change in PSS suppliers. Distribution options could involve the use of alternative raw materials such as low-kaolinite metakaolin that could be produced from clays with a high content of kaolinite [59]—an abundant resource often available locally in France [60]. Freight by train or by barge could also be envisioned to further decrease transport impacts. This represents an important research perspective of this work.

### 4.2. Matrix Optimization

The geopolymer matrix formulation was selected based on its mechanical performance and its climate change impact. This procedure could be further deployed to evaluate candidates in all environmental impact categories. The authors want to highlight the methodology set up to develop the geopolymer, which is simplified and restrained to one single indicator in the first step for readability. They acknowledge the importance of the multi-criteria approach in LCA.

The LCA results also showed that the formulation with sand (GP-S) exhibits better results than the formulation with earth (GP-SE). The use of locally excavated earth could,

however, be beneficial as a strategy to reduce impacts related to the extraction of sand in the context of aggregate scarcity and a lack of environmental regulation [7,8].

Moreover, the use of sodium instead of potassium in the alkaline solution could also produce geopolymers suited for structural applications while reducing both the cost and the environmental burden [9]. Other synthesis processes could be investigated in a future study to use broadly available potash salts instead of potassium hydroxide in the confection of potassium silicate solution (waterglass).

Finally, the printability of the formulation has been measured in a simple way, even if better methods exist, like the squeeze test [61] or modified Vicat [62], for instance. In [63], we developed an original and efficient in-line test for 3D concrete, the slug test, which is able to deduce the yield stress from the weight of drops falling from the nozzle, which directly relies on the printability. In [36], we successfully adopted this method for the GP-GfW geopolymer used in this study for comparisons, and future tests will be conducted for the formulations integrating earth, to confirm their printability.

#### 4.3. Uncertainties

Uncertainty values are high, as the data suffers from some severe flaws, especially in foreground processes. The estimation of this uncertainty is a critical issue for comprehensive LCA results [64]. For PSS, the data on potassium are inexistent, following an existing trend in the chemical industry [65]. The values for alkali silicates come from a 25-year-old study from Fawer and colleagues [45], as is the case in the vast majority of other LCA studies such as [19,22,66]. It strongly affects the temporal and technological correlation parameters and consequently gives high uncertainty to the related process. For MK, the material comes from widely different processes, and a high variability is observed in the literature [19,22,66]. Consequently, the technological correlation is low. Furthermore, an uncertainty assessment is not explained in this article, although it is considered to be a major perspective of this work.

The uncertainty related to the freshwater ecotoxicity indicator will hopefully soon be reduced with ongoing work on improving the characterization factor of metals. In the meantime, this result has to be taken with caution. For instance, the most important contributing elementary flows differ between the ILCD and Impact World+ indicators [67], with questions on both results and the overall contribution of this category in the environmental assessment of GP mortar.

#### 4.4. Damage Assessment Method

As endpoint characterization methods are subject to higher uncertainties than the midpoint, a sensitivity analysis was performed using another method: ImpactWorld+ [67]. The results significantly differ, especially for biodiversity assessment and the contribution of long-term effects regarding freshwater ecotoxicity, which clearly dominates the ImpactWorld+ results. This impact category is subject to very high uncertainties, and this result is the consequence of only a few compounds highly persistent in the environment. Here, these are aluminum, copper, and iron, which come from upstream secondary processes related to sulfidic tailing from copper production. There is an important debate on ecotoxicity characterization factors for metals, which could eventually lead to a decrease in their contribution by at least two orders of magnitude [68,69]. There is also a current debate on the possible overestimation of tailing releases to the environment [70]. Excluding long-term effects to avoid this metal issue, the dominant category is climate change, closely followed by land use (related to transport) and acidification. Details on stressor contribution to freshwater ecotoxicity impacts are available in Supplementary Materials, Section S3.

The ReCiPe2016 method, a hierarchist scenario, used in this work does not consider the long-term effects of ecotoxicity (over 100 years), which could potentially lead to an underestimation of the impacts of very persistent compounds. However, stressor contribution results were consistent with the ILCD method used for midpoint assessment. Uncertain impacts must be assessed even if uncertain and ongoing important research efforts might

soon lead to a better comprehension of occurring phenomena and a reduction of related uncertainties and variations among models.

#### 4.5. Comparative LCA with 3D Printing Mortar Based on OPC

For simplicity reasons, the choice of a conventional equivalent was based on concrete with 100% OPC. Although 100% OPC is still widely used, a wide range of alternative clinkers have been developed [71]. It would be highly consistent to further include the proposed geopolymer in a wider perspective, comparing it to a wide scope of 3D-printing materials.

### 5. Conclusions and Perspective

The research presented in this paper focuses on geopolymer compositions iteratively developed for structural applications, with the goal of lowering the environmental impact. An LCA model for MK- and PSS-based geopolymer mortars was built. This model was used to optimize the GP matrix and granular skeleton starting from an existing formulation, through the reduction of GHG emissions. Two optimized formulations of GP mortars suitable for 3D printing were then compared with a 3D-printed mortar based on Portland cement. The results were completed by a sensitivity analysis of the transport of raw materials. The conclusions of this LCA show that 3D-printed GP formulations are not yet a mature technology, and short-term applications of this technology are not necessarily environmentally beneficial. Nevertheless, GPs hold great potential as they can divide GHG emissions by a factor close to two, with conceivable innovations. In the meantime, human and environmental toxicities, mineral depletion, and fossil resources are increased by the GP mortars—a trade-off already underlined by previous studies. The designed material shows good extrudability and buildability and could be used in high-performance applications thanks to its high compressive strength. Despite its low proportion of aggregates, this material displays significant environmental assets as it contains an important share of earth that is widely available and often treated as waste.

Some other prospective works lie ahead and are worth exploring. First, there is a need for a prospective resource-availability assessment for the GP technology (alkali, kaolin clays) to ensure that the required resources are widely available or to define locations that could most benefit from the technology. Secondly, an environmental assessment of the large-scale use of 3D printing in building applications must be conducted, as the literature is still scarce. A robust uncertainty assessment should be undertaken with rigorous sampling for processes specific to geopolymers. Furthermore, the social impact of such a new technique is also worth exploring before its wider application.

**Supplementary Materials:** The following supporting information can be downloaded at: <https://www.mdpi.com/article/10.3390/su16083328/s1>. Section S1: Process of Detailed Modelization; Section S2: Impact Categories; Section S3: LCA Results: Stressor Contribution to Ecotoxicity.

**Author Contributions:** C.R.: Conceptualization, Writing—Original draft preparation, visualization, validation—environmental assessment part; J.A.: Conceptualization, Writing—Original draft preparation, Visualization, validation—mechanical and workability characterization part; C.L.G.: Conceptualization, Methodology, Investigation, Software; M.S.: Writing—Original draft preparation, Critical Review and Editing, A.F.: Writing—Review and Editing, supervision; J.-F.C.: Writing—Review and Editing, supervision, Project administration, funding acquisition. All authors have read and agreed to the published version of the manuscript.

**Funding:** This work was performed using the funds of the NAVIER research lab.

**Informed Consent Statement:** Not applicable.

**Data Availability Statement:** Data is contained within the article or Supplementary Materials. A dataset for more detailed information is available on request from the authors.

**Conflicts of Interest:** The authors declare no conflicts of interest.

## References

1. Miller, S.A.; Moore, F.C. Climate and health damages from global concrete production. *Nat. Clim. Chang.* **2020**, *10*, 439–443. [CrossRef]
2. Shi, C.; Jiménez, A.F.; Palomo, A. New cements for the 21st century: The pursuit of an alternative to Portland cement. *Cem. Concr. Res.* **2011**, *41*, 750–763. [CrossRef]
3. Habert, G.; Miller, S.A.; John, V.M.; Provis, J.L.; Favier, A.; Horvath, A.; Scrivener, K.L. Environmental impacts and decarbonization strategies in the cement and concrete industries. *Nat. Rev. Earth Environ.* **2020**, *1*, 559–573. [CrossRef]
4. Makul, N. Modern sustainable cement and concrete composites: Review of current status, challenges and guidelines. *Sustain. Mater. Technol.* **2020**, *25*, e00155. [CrossRef]
5. Sivakrishna, A.; Adesina, A.; Awoyera, P.O.; Rajesh Kumar, K. Green concrete: A review of recent developments. *Mater. Today Proc.* **2020**, *27*, 54–58. [CrossRef]
6. Van Deventer, J.S.J.; Provis, J.L.; Duxson, P. Technical and commercial progress in the adoption of geopolymer cement. *Miner. Eng.* **2012**, *29*, 89–104. [CrossRef]
7. UNEP. *Sand and Sustainability: Finding New Solutions for Environmental Governance of Global Sand Resources*; GRID-Geneva, United Nations Environment Programme: Geneva, Switzerland, 2019; Available online: [https://unepgrid.ch/storage/app/media/documents/Sand\\_and\\_sustainability\\_UNEP\\_2019.pdf](https://unepgrid.ch/storage/app/media/documents/Sand_and_sustainability_UNEP_2019.pdf) (accessed on 26 March 2021).
8. Bendixen, M.; Best, J.; Hackney, C.; Iversen, L.L. Time is running out for sand. *Nature* **2019**, *571*, 29–31. [CrossRef] [PubMed]
9. Davidovits, J. *Geopolymer Chemistry and Applications*; Geopolymer Institute: Saint-Quentin, France, 2008; ISBN 978-2-9514820-1-2.
10. Zhang, P.; Zheng, Y.; Wang, K.; Zhang, J. A review on properties of fresh and hardened geopolymer mortar. *Compos. Part B Eng.* **2018**, *152*, 79–95. [CrossRef]
11. Amran, Y.H.M.; Alyousef, R.; Alabduljabbar, H.; El-Zeadani, M. Clean production and properties of geopolymer concrete; A review. *J. Clean. Prod.* **2020**, *251*, 119679. [CrossRef]
12. Pradhan, P.; Dwibedy, S.; Pradhan, M.; Panda, S.; Panigrahi, S.K. Durability characteristics of geopolymer concrete—Progress and perspectives. *J. Build. Eng.* **2022**, *59*, 105100. [CrossRef]
13. Monteiro, P.J.M.; Miller, S.A.; Horvath, A. Towards sustainable concrete. *Nat. Mater.* **2017**, *16*, 698–699. [CrossRef] [PubMed]
14. Provis, J.L. Green concrete or red herring?—Future of alkali-activated materials. *Adv. Appl. Ceram.* **2014**, *113*, 472–477. [CrossRef]
15. Curran, M.A. *Life Cycle Assessment Handbook: A Guide for Environmentally Sustainable Products*; John Wiley & Sons: Hoboken, NJ, USA, 2012; ISBN 978-1-118-52841-9.
16. Guinée, J.B.; Lindeijer, E. *Handbook on Life Cycle Assessment: Operational Guide to the ISO Standards*; Springer Science & Business Media: Berlin/Heidelberg, Germany, 2002; ISBN 978-1-4020-0228-1.
17. Ghadir, P.; Zamanian, M.; Mahbubi-Motlagh, N.; Saberian, M.; Li, J.; Ranjbar, N. Shear strength and life cycle assessment of volcanic ash-based geopolymer and cement stabilized soil: A comparative study. *Transp. Geotech.* **2021**, *31*, 100639. [CrossRef]
18. Meshram, R.B.; Kumar, S. Comparative life cycle assessment (LCA) of geopolymer cement manufacturing with Portland cement in Indian context. *Int. J. Environ. Sci. Technol.* **2022**, *19*, 4791–4802. [CrossRef]
19. Habert, G.; d’Espinoze de Lacaillerie, J.B.; Roussel, N. An environmental evaluation of geopolymer based concrete production: Reviewing current research trends. *J. Clean. Prod.* **2011**, *19*, 1229–1238. [CrossRef]
20. Weil, M.; Dombrowski, K.; Buchwald, A. 10—Life-cycle analysis of geopolymers. In *Geopolymers*; Provis, J.L., van Deventer, J.S.J., Eds.; Woodhead Publishing: Sawston, UK, 2009; pp. 194–210. ISBN 978-1-84569-449-4.
21. Matheu, P.S.; Ellis, K.; Varela, B. Comparing the Environmental Impacts of Alkali Activated Mortar and Traditional Portland Cement Mortar using Life Cycle Assessment. *IOP Conf. Ser. Mater. Sci. Eng.* **2015**, *96*, 012080. [CrossRef]
22. Heath, A.; Paine, K.; McManus, M. Minimising the global warming potential of clay based geopolymers. *J. Clean. Prod.* **2014**, *78*, 75–83. [CrossRef]
23. Davidovits, J. False Values on CO2 Emission for Geopolymer Cement/Concrete, Scientific Papers, Technical Paper #24, Geopolymer Institute Library. 2015. Available online: <http://www.geopolymer.org/wp-content/uploads/False-CO2-values.pdf> (accessed on 2 September 2021).
24. Yao, Y.; Hu, M.; Maio, F.D.; Cucurachi, S. Life cycle assessment of 3D printing geo-polymer concrete: An ex-ante study. *J. Ind. Ecol.* **2020**, *24*, 116–127. [CrossRef]
25. Morel, J.-C.; Charef, R.; Hamard, E.; Fabbri, A.; Beckett, C.; Bui, Q.-B. Earth as construction material in the circular economy context: Practitioner perspectives on barriers to overcome. *Philos. Trans. R. Soc. B Biol. Sci.* **2021**, *376*, 20200182. [CrossRef]
26. Luzu, B.; Duc, M.; Djerbi, A.; Gautron, L. High Performance Illitic Clay-Based Geopolymer: Influence of the Mechanochemical Activation Duration on the Strength Development. In *Calcined Clays for Sustainable Concrete*; Bishnoi, S., Ed.; Springer: Singapore, 2020; pp. 363–373.
27. Essaidi, N.; Samet, B.; Baklouti, S.; Rossignol, S. Feasibility of producing geopolymers from two different Tunisian clays before and after calcination at various temperatures. *Appl. Clay Sci.* **2014**, *88–89*, 221–227. [CrossRef]
28. De Schutter, G.; Lesage, K.; Mechtcherine, V.; Nerella, V.N.; Habert, G.; Agusti-Juan, I. Vision of 3D printing with concrete—Technical, economic and environmental potentials. *Cem. Concr. Res.* **2018**, *112*, 25–36. [CrossRef]
29. Song, R.; Wang, Y.; Ishutov, S.; Zambrano-Narvaez, G.; Hodder, K.J.; Chalaturnyk, R.J.; Sun, S.; Liu, J.; Gamage, R.P. A Comprehensive Experimental Study on Mechanical Behavior, Microstructure and Transport Properties of 3D-printed Rock Analogs. *Rock. Mech. Rock. Eng.* **2020**, *53*, 5745–5765. [CrossRef]

30. Hassan, A.; Arif, M.; Shariq, M. Use of geopolymer concrete for a cleaner and sustainable environment—A review of mechanical properties and microstructure. *J. Clean. Prod.* **2019**, *223*, 704–728. [[CrossRef](#)]
31. Singh, B.; Ishwarya, G.; Gupta, M.; Bhattacharyya, S.K. Geopolymer concrete: A review of some recent developments. *Constr. Build. Mater.* **2015**, *85*, 78–90. [[CrossRef](#)]
32. Zakka, W.P.; Abdul Shukor Lim, N.H.; Chau Khun, M. A scientometric review of geopolymer concrete. *J. Clean. Prod.* **2021**, *280*, 124353. [[CrossRef](#)]
33. Komnitsas, K. Potential of geopolymer technology towards green buildings and sustainable cities. *Procedia Eng.* **2011**, *21*, 1023–1032. [[CrossRef](#)]
34. Zhong, H.; Zhang, M. 3D printing geopolymers: A review. *Cem. Concr. Compos.* **2022**, *128*, 104455. [[CrossRef](#)]
35. Turner, L.K.; Collins, F.G. Carbon dioxide equivalent (CO<sub>2</sub>-e) emissions: A comparison between geopolymer and OPC cement concrete. *Constr. Build. Mater.* **2013**, *43*, 125–130. [[CrossRef](#)]
36. Archez, J.; Maitenaz, S.; Demont, L.; Charrier, M.; Mesnil, R.; Texier-Mandoki, N.; Bourbon, X.; Rossignol, S.; Caron, J.F. Strategy to shape, on a half-meter scale, a geopolymer composite structure by additive manufacturing. *Open Ceram.* **2021**, *5*, 100071. [[CrossRef](#)]
37. *NF-EN 197-1*; Cement—Part 1: Composition, Specifications and Conformity Criteria for Common Cements. NFE: Paris, France, 2001.
38. Archez, J.; Texier-Mandoki, N.; Bourbon, X.; Caron, J.F.; Rossignol, S. Adaptation of the geopolymer composite formulation binder to the shaping process. *Mater. Today Commun.* **2020**, *25*, 101501. [[CrossRef](#)]
39. Gökçe, H.S.; Tuyan, M.; Nehdi, M.L. Alkali-activated and geopolymer materials developed using innovative manufacturing techniques: A critical review. *Constr. Build. Mater.* **2021**, *303*, 124483. [[CrossRef](#)]
40. Archez, J.; Texier-Mandoki, N.; Bourbon, X.; Caron, J.F.; Rossignol, S. Shaping of geopolymer composites by 3D printing. *J. Build. Eng.* **2021**, *34*, 101894. [[CrossRef](#)]
41. Mutel, C. Brightway: An open source framework for Life Cycle Assessment. *JOSS* **2017**, *2*, 236. [[CrossRef](#)]
42. Steubing, B.; de Koning, D.; Haas, A.; Mutel, C.L. The Activity Browser—An open source LCA software building on top of the brightway framework. *Softw. Impacts* **2020**, *3*, 100012. [[CrossRef](#)]
43. Frischknecht, R.; Jungbluth, N.; Althaus, H.-J.; Doka, G.; Dones, R.; Heck, T.; Hellweg, S.; Hischier, R.; Nemecek, T.; Rebitzer, G.; et al. The ecoinvent Database: Overview and Methodological Framework (7 pp). *Int. J. Life Cycle Assess.* **2005**, *10*, 3–9. [[CrossRef](#)]
44. Wernet, G.; Bauer, C.; Steubing, B.; Reinhard, J.; Moreno-Ruiz, E.; Weidema, B. The ecoinvent database version 3 (part I): Overview and methodology. *Int. J. Life Cycle Assess.* **2016**, *21*, 1218–1230. [[CrossRef](#)]
45. Fawer, M.; Concannon, M.; Rieber, W. Life cycle inventories for the production of sodium silicates. *Int. J. LCA* **1999**, *4*, 207. [[CrossRef](#)]
46. Chomkham Sri, K.; Wolf, M.-A.; Pant, R. International Reference Life Cycle Data System (ILCD) Handbook: Review Schemes for Life Cycle Assessment. In *Towards Life Cycle Sustainability Management*; Finkbeiner, M., Ed.; Springer: Amsterdam, The Netherlands, 2011; pp. 107–117. ISBN 978-94-007-1898-2.
47. Saouter, E.; Biganzoli, F.; Ceriani, L.; Versteeg, D.; Crenna, E.; Zampori, L.; Sala, S.; Pant, R. *Environmental Footprint: Update of Life Cycle Impact Assessment Methods: Ecotoxicity Freshwater, Human Toxicity Cancer, and Non Cancer*; Publications Office of the European Union: Luxembourg, 2020; ISBN 978-92-76-17143-0.
48. Huijbregts, M.A.J.; Steinmann, Z.J.N.; Elshout, P.M.F.; Stam, G.; Verones, F.; Vieira, M.; Zijp, M.; Hollander, A.; van Zelm, R. ReCiPe2016: A harmonised life cycle impact assessment method at midpoint and endpoint level. *Int. J. Life Cycle Assess.* **2017**, *22*, 138–147. [[CrossRef](#)]
49. Huijbregts, M.A.J.; Rombouts, L.J.A.; Hellweg, S.; Frischknecht, R.; Hendriks, A.J.; van de Meent, D.; Ragas, A.M.J.; Reijnders, L.; Struijs, J. Is Cumulative Fossil Energy Demand a Useful Indicator for the Environmental Performance of Products? *Environ. Sci. Technol.* **2006**, *40*, 641–648. [[CrossRef](#)]
50. Gharzouni, A.; Sobrados, I.; Balouti, S.; Joussein, E.; Rossignol, S. Control of polycondensation reaction generated from different metakaolins and alkaline solutions. *J. Ceram. Sci. Technol.* **2017**, *8*, 365–376.
51. Jaya, N.A.; Liew, Y.M.; Heah, C.Y.; Abdullah, M.M.A.B. Effect of solid-to-liquid ratios on metakaolin geopolymers. *AIP Conf. Proc.* **2018**, *2045*, 020099. [[CrossRef](#)]
52. Roussel, N. Rheological requirements for printable concretes. *Cem. Concr. Res.* **2018**, *112*, 76–85. [[CrossRef](#)]
53. Romagnoli, M.; Leonelli, C.; Kamse, E.; Lassinantti Gualtieri, M. Rheology of geopolymer by DOE approach. *Constr. Build. Mater.* **2012**, *36*, 251–258. [[CrossRef](#)]
54. Kuzmenko, K.; Roux, C.; Feraille, A.; Baverel, O. Assessing environmental impact of digital fabrication and reuse of constructive systems. *Structures* **2021**, *31*, 1300–1310. [[CrossRef](#)]
55. Agustí-Juan, I.; Habert, G. An Environmental Perspective on Digital Fabrication in Architecture and Construction. In Proceedings of the 21st International Conference on Computer-Aided Architectural Design Research in Asia (Caadria 2016), Melbourne, Australia, 30 March–2 April 2016; pp. 797–806. Available online: [http://papers.cumincad.org/data/works/att/caadria2016\\_797.pdf](http://papers.cumincad.org/data/works/att/caadria2016_797.pdf) (accessed on 7 May 2021).
56. Agustí-Juan, I.; Müller, F.; Hack, N.; Wangler, T.; Habert, G. Potential benefits of digital fabrication for complex structures: Environmental assessment of a robotically fabricated concrete wall. *J. Clean. Prod.* **2017**, *154*, 330–340. [[CrossRef](#)]
57. San Nicolas, R.; Cyr, M.; Escadeillas, G. Characteristics and applications of flash metakaolins. *Appl. Clay Sci.* **2013**, *83–84*, 253–262. [[CrossRef](#)]

58. Deteuf, C. Imerys Metakaolin Production.pdf. 2016. Available online: <https://geopolymer.org/fichiers/gpcamp-2016/Deteuf%20-%20Imerys%20metakaolin%20production.pdf> (accessed on 23 September 2021).
59. Batis, G.; Pantazopoulou, P.; Tsivilis, S.; Badogiannis, E. The effect of metakaolin on the corrosion behavior of cement mortars. *Cem. Concr. Compos.* **2005**, *27*, 125–130. [[CrossRef](#)]
60. Handbook on Kaolin and Kaolinic Clays | BRGM. Available online: <https://www.brgm.fr/en/reference-completed-project/handbook-kaolin-kaolinic-clays> (accessed on 7 April 2023).
61. Toutou, Z.; Roussel, N.; Lanos, C. The squeezing test: A tool to identify firm cement-based material's rheological behaviour and evaluate their extrusion ability. *Cem. Concr. Res.* **2005**, *35*, 1891–1899. [[CrossRef](#)]
62. Sleiman, H.; Perrot, A.; Amziane, S. A new look at the measurement of cementitious paste setting by Vicat test. *Cem. Concr. Res.* **2010**, *40*, 681–686. [[CrossRef](#)]
63. Ducoulombier, N.; Mesnil, R.; Carneau, P.; Demont, L.; Bessaies-Bey, H.; Caron, J.-F.; Roussel, N. The “Slugs-test” for extrusion-based additive manufacturing: Protocol, analysis and practical limits. *Cem. Concr. Compos.* **2021**, *121*, 104074. [[CrossRef](#)]
64. Heijungs, R.; Huijbregts, M.A. A Review of Approaches to Treat Uncertainty in LCA. 2004. Available online: <http://scholarsarchive.byu.edu/iemssconference/2004/all/197/> (accessed on 7 September 2017).
65. Oberschelp, C.; Hellweg, S.; Bradford, E.; Pfister, S.; Huo, J.; Wang, Z. Poor Data and Outdated Methods Sabotage the Decarbonization Efforts of the Chemical Industry. 2023. Available online: <https://doi.org/10.26434/chemrxiv-2023-8c86t> (accessed on 25 May 2023).
66. Shobeiri, V.; Bennett, B.; Xie, T.; Visintin, P. A comprehensive assessment of the global warming potential of geopolymer concrete. *J. Clean. Prod.* **2021**, *297*, 126669. [[CrossRef](#)]
67. Bulle, C.; Margni, M.; Patouillard, L.; Boulay, A.-M.; Bourgault, G.; De Bruille, V.; Cao, V.; Hauschild, M.; Henderson, A.; Humbert, S.; et al. IMPACT World+: A globally regionalized life cycle impact assessment method. *Int. J. Life Cycle Assess.* **2019**, *24*, 1653–1674. [[CrossRef](#)]
68. Hedberg, J.; Fransson, K.; Prideaux, S.; Roos, S.; Jönsson, C.; Odnevall Wallinder, I. Improving the Life Cycle Impact Assessment of Metal Ecotoxicity: Importance of Chromium Speciation, Water Chemistry, and Metal Release. *Sustainability* **2019**, *11*, 1655. [[CrossRef](#)]
69. Gandhi, N.; Diamond, M.L. Freshwater ecotoxicity characterization factors for aluminum. *Int. J. Life Cycle Assess.* **2018**, *23*, 2137–2149. [[CrossRef](#)]
70. Muller, S.; Lassin, A.; Lai, F.; Thiéry, D.; Guignot, S. Modelling releases from tailings in life cycle assessments of the mining sector: From generic models to reactive transport modelling. *Miner. Eng.* **2022**, *180*, 107481. [[CrossRef](#)]
71. Gartner, E.; Sui, T. Alternative cement clinkers. *Cem. Concr. Res.* **2018**, *114*, 27–39. [[CrossRef](#)]

**Disclaimer/Publisher's Note:** The statements, opinions and data contained in all publications are solely those of the individual author(s) and contributor(s) and not of MDPI and/or the editor(s). MDPI and/or the editor(s) disclaim responsibility for any injury to people or property resulting from any ideas, methods, instructions or products referred to in the content.